08

Features of magnetic behavior of nanomaterials based on bismuth ferrites

© N.A. Lomanova, S.G. Yastrebov

Ioffe Institute,
St. Petersburg, Russia

E-mail: natus@mail.ioffe.ru

Received April 30, 2024
Revised October 28, 2024
Accepted October 30, 2024

The magnetic properties of nanocrystalline materials based on perovskite-like ($BiFeO_3$) and mullite-like ($Bi_2Fe_4O_9$) bismuth ferrites have been studied. The $BiFeO_3$ and $Bi_2Fe_4O_9$ samples have been synthesized by solution combustion and have average crystallite sizes of 48 ± 2 and 60 ± 3 nm, respectively. At room temperature, they are in a magnetically ordered state and have a higher total magnetization compared to the literature data on nanomaterials of similar composition, which is higher for $Bi_2Fe_4O_9$. Both materials have a similar type of experimental dependences of magnetization on temperature. It is demonstrated that the Hill model accurately describes the temperature behavior of magnetization and is of interest for predicting the properties of bismuth ferrite-based materials in the development of promising magnetic media.

Keywords: bismuth orthoferrite, nanocrystals, glycine-nitrate combustion, magnetic properties.

DOI: 10.61011/PSS.2024.12.60186.6517PA

1. Introduction

Ferrites of bismuth, $BiFeO_3$ and $Bi_2Fe_4O_9$, are of interest for various fields of nanoelectronics, since are semiconductors, promising magnetic materials, in particular, multiferroics. It is important that perovskite-like bismuth orthoferrite ($BiFeO_3$) — high-temperature multiferroic with temperature of transition to magnetic-ordered state above room temperature (Neel temperature $T_N = 640$ K [1]), which makes it possible to use this material under normal conditions.

Bulk $BiFeO_3$ is antiferromagnetic and has a spatial modulation of magnetization (a spin cycloid with $\lambda_C = 62$ nm period), the suppression of which is one of the important technological problems and occurs, in particular, with reduction of particle sizes [2,3]. Bismuth ferrite $Bi_2Fe_4O_9$ has mullite-like structure and in the volume form below room temperature is antiferromagnetic with $T_N = 237-265$ K [4]. Weak ferromagnetism in these materials arises due to a taper in the antiferromagnetic sublattice of iron and implementation of Dzyaloshinski-Moriya exchange interaction [5,6].

Many papers exist on prospects of using nanomaterials based on bismuth ferrites (see review [2] and references therein). In the nanosize form these materials have higher magnetic response [3,7,8]. This is due to size and surface effects in nanocrystals that manifest itself in the increase of total magnetization due to tapering of spins on the particle surface.

When transferring to nanosize region, the role of size and surface effects of nanoparticles that greatly influence the properties and depend on the technology of these materials manufacturing increases [2,3,8]. Such capabilities as functional response control, in particular, magnetic behavior of bismuth ferrites [8], by changing composition, morphology and chemical pre-history of the initial composition, enables active development of this area of material science for decades.

Study of the temperature behavior of magnetization is important to understand the processes happening in these materials, since it opens the opportunity to control the magnetic characteristics to the temperatures exceeding the room one. The objective of the paper was to study magnetic characteristics of nanocrystalline bismuth ferrites, $BiFeO_3$ and $Bi_2Fe_4O_9$, and to analyze the obtain data using the theoretical model, making it possible to predict the temperature behavior of the bismuth ferrite magnetization with different structures.

2. Synthesis and characterization

Samples of $BiFeO_3$ and $Bi_2Fe_4O_9$ were synthesized by glycine-nitrate combustion method. The synthesis technique was detailed in papers [7–9]. The phase composition of the samples was determined on Rigaku SmartLab 3 diffractometer (Cu$K\alpha$-radiation). X-ray diffraction patterns of the samples are shown in Figure 1, *a*. According to XPA data, the main products in the samples are isostructural to the rhombohedral phase of $BiFeO_3$ (PDF 14-181) and orthorhombic phase of $Bi_2Fe_4O_9$ (PDF 25-90), no admixture phases were recorded. The average crystallite size determined from the main reflexes of $BiFeO_3$ (012/110) and $Bi_2Fe_4O_9$ (121/211), is given in Figure 1, *a*. Distribution of crystallites by size was determined in the approximation

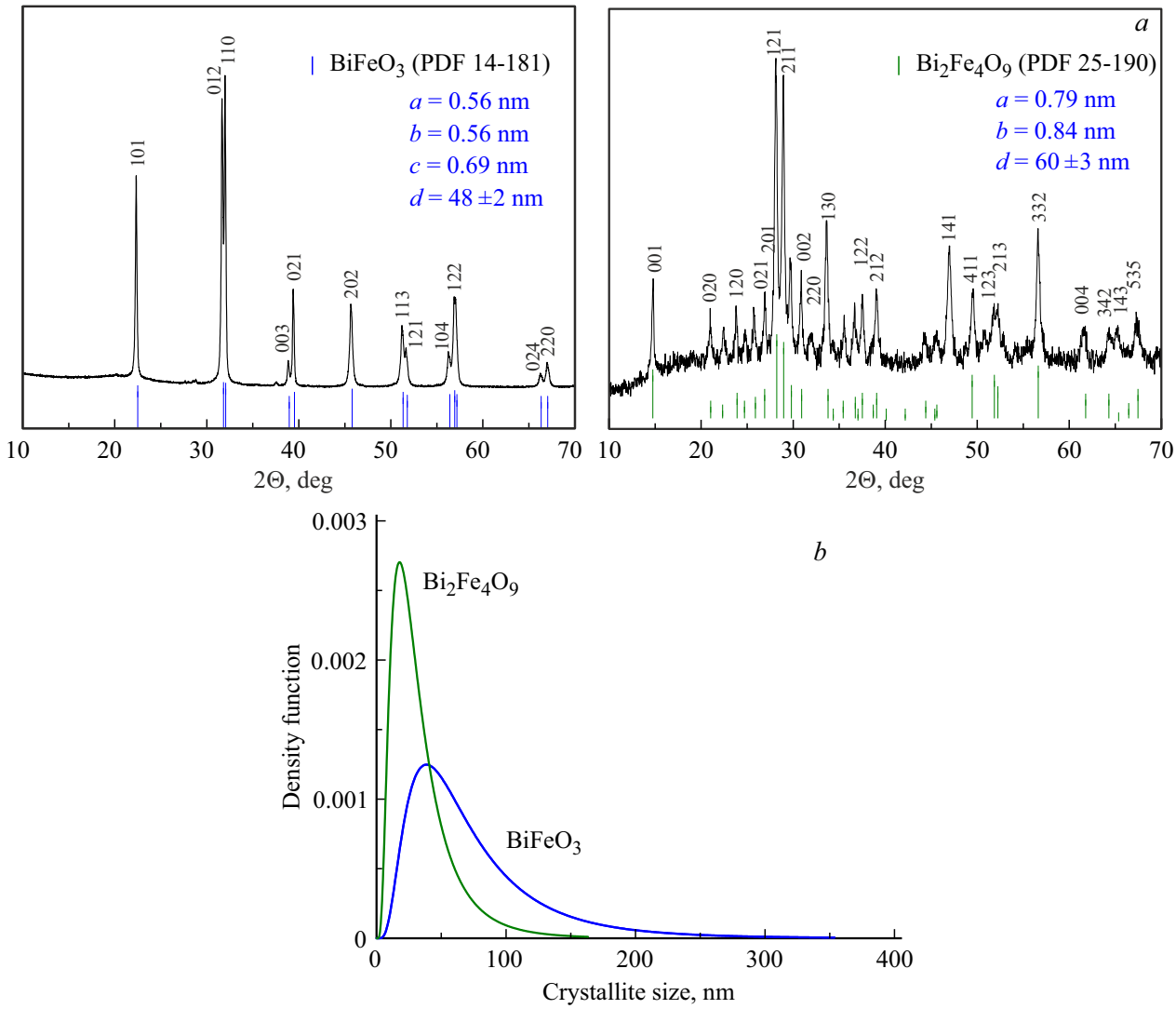

Figure 1. X-ray diffraction patterns (*a*) and distribution of crystallites by dimensions (*b*).

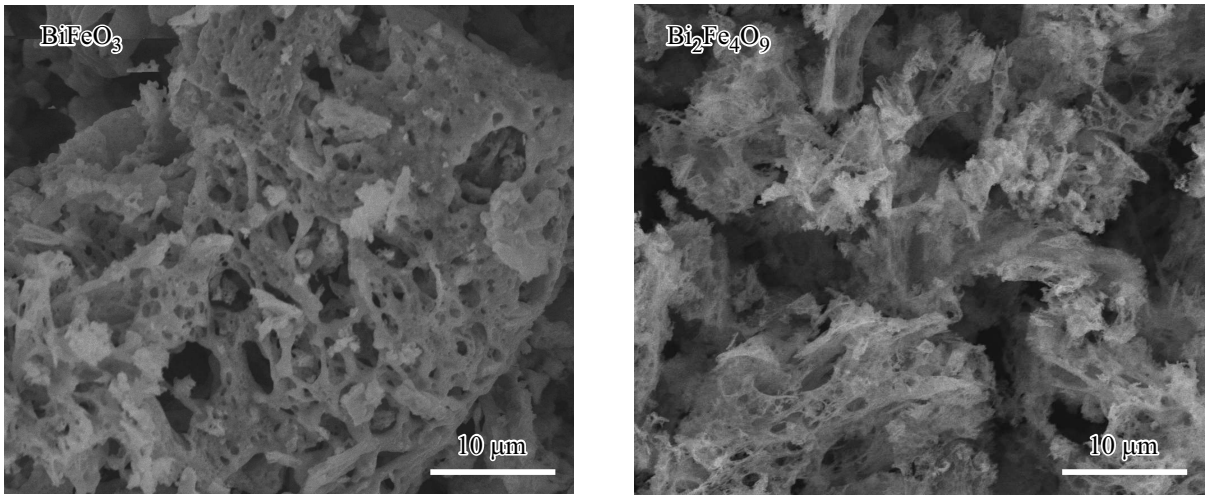

Figure 2. SEM-images of produced materials.

of the lognormal distribution law in software complex SmartLab using Halder-Wagner model and is given in Figure 1, *b*. The microstructure of the produced materials is given in Figure 2 and was defined on scanning electron microscope FEI Quanta 200. It was found that the produced powders were porous aggregates of particles formed as a result of intensive gas formation from combustion of source compositions.

The field and temperature dependences of magnetization M were measured on a vibration magnetometer of PPMS system (Quantum Design). Dependences $M(H)$ were determined at 300 K. Dependences $M(T)$ were measured at the external magnetic field 100 Oe.

3. Magnetic study results

Magnetization curves $M(H)$ of both materials presented in Figure 3, have hysteresis at room temperature, which indicates their magnetic-ordered state. The form of hysteresis loop $BiFeO_3$ has the appearance of „wasp waist". Such type is specific for a mix of multi-domain and single-domain particles with the prevalent multi-domain phase [10], which correlates with the particle distribution by size (Figure 1, *b*).

Curves $M(H)$ do not achieve saturation, even though curve $BiFeO_3$ is close thereto, which indicates a superparamagnetic contribution to the total magnetic response of samples. As the distribution of crystallites by size shows (Figure 1, *b*), powders are an ensemble of nanoparticles with various dispersity. Finely dispersed fraction in the samples may be formed either by substance of X-ray amorphous part of synthesis products or by areas of particle surfaces. Non-saturating behavior of the loop provides for the presence of competing antiferromagnetic interactions in nanoparticles of bismuth ferrites, having an ordered AFM-nucleus and non-compensated spins on the surface [11].

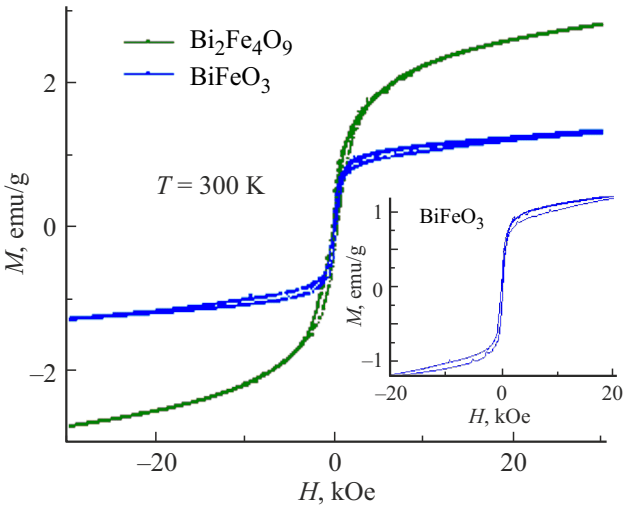

Figure 3. Dependences of magnetization M of samples on external magnetic field H. The insert contains curve $M(H)$ $BiFeO_3$, measured at 300 K in small fields.

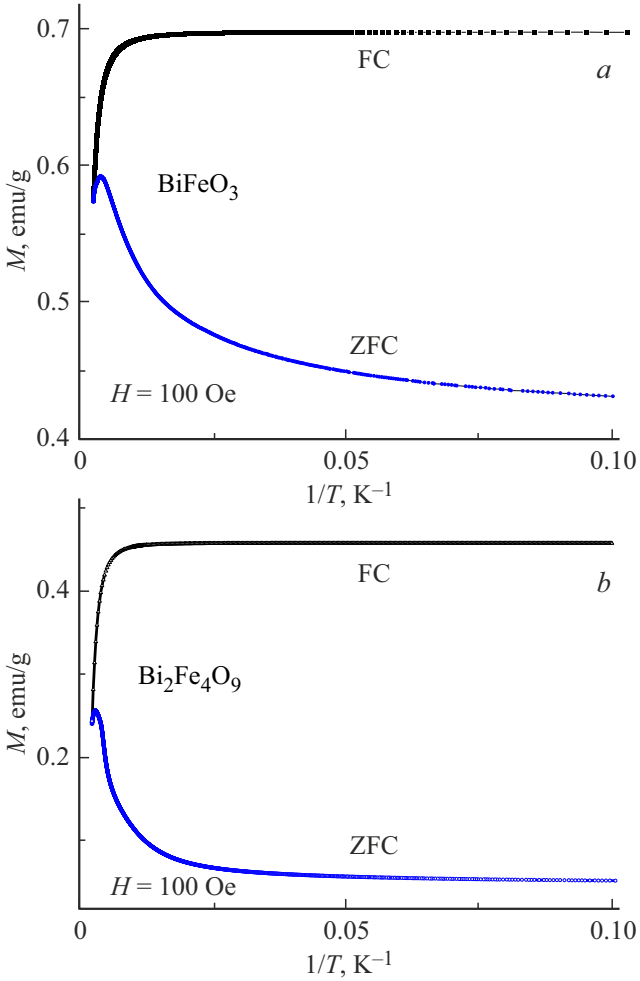

Figure 4. Dependences of magnetization of samples $BiFeO_3$ (*a*) and $Bi_2Fe_4O_9$ (*b*) on opposite temperature.

One can see that the sample $BiFeO_3$ has lower total magnetization compared to the second sample. Apart from the effect of the composition (smaller number of magnetic cations), the weaker magnetic response of sample $BiFeO_3$ is related to the presence of a spin cycloid that suppresses magnetization. Even though, as it is shown in the previous paper [12], this magnetic structure is preserved in nanoparticles of bismuth orthoferrite with the average size of crystallites $d > \lambda c$, since there is particle distribution by size. It should be noted that value M of both samples is higher compared to materials of similar composition with close values d, specified in papers [3,13,14] at the same value H. High values M in such samples are usually recorded at particle size below 15–20 nm [3,15]. In our experiment at 300 K and 20 kOe the values $M = 1.2$ and 2.5 emu/g were recorded for $BiFeO_3$ and $Bi_2Fe_4O_9$, accordingly.

Figure 4 shows temperature dependences of sample magnetization built for more detailed discussion, in Arrhenius coordinates. One can see that for materials of various structures the trend of experimental dependences of mag-

netization is similar and may be described within a single theoretical model. Curves FC/ZFC have typical divergence for nanopowders near the low argument values (around room temperature). It was found that FC curves could be effectively approximated using Hill function (1). Such coincidence seems obvious, since the process of magnetization variation depends on the temperature and interaction of adjacent nanoparticles that reminds of formation and break of a bond between the closest adjacent pellets, which is also typical for some biological objects. Adjustment parameters in this case may be used for quantitative characterization of magnetic properties of various composition

$$M(x) = M_m \frac{x^n}{k^n + x^n}, \quad (1)$$

where M — magnetization, M_m — maximum value achieved M with temperature growth, $x = 1/T$ — opposite temperature, n — Hill ratio, k — constant determining function value at half of its height.

FC curve of sample $BiFeO_3$ (Figure 4, *a*) is approximated by Hill model with the following set of parameters: $M_m = 0.7$, $k = 0.001$, $n = 2.32$. For sample $Bi_2Fe_4O_9$ (Figure 4, *b*) the following parameters are used: $M_m = 0.46$, $k = 0.002$, $n = 3.29$. One can see that the high value M_m with temperature increase is achieved in the material based on $BiFeO_3$, having lower average value d. At the same time, for this sample a lower value n is also specific, which characterizes the formation of the total magnetic response and sharp drop of FC/ZFC magnetization with temperature growth as a result of the fact that the material contains more unrelated magnetic moments. This is matched with its wider distribution of crystallites by size (Figure 1, *b*), indicating that sample $BiFeO_3$ contains more ultradisperse fraction.

The trend of FC curves shows that the magnetic field orders magnetic moments of particles and they are built in the field. Temperature has disordering effect on the total magnetic moment in the local environment of larger particles. As the opposite temperature reduces further, the effect of disordering of magnetic moments orientation arises, which causes lower magnetization.

The behavior of ZFC curves shows that in the low-temperature region the neighboring interacting particles are in a state with minimum energy, i. e. their total magnetic moments are compensated (antiparallel orientation). As temperature increases, magnetic moments of smaller size particles are disordered, and the total magnetization of the nanoparticle ensemble increases.

ZFC-dependences, built in the Arrhenius coordinates, are far from linearity, which indicates non-linear nature of interaction of the neighboring nanoparticles. For both samples these dependences achieve the maximum in the area of low argument values, i. e. high temperatures. As temperature increases further, dependences drop. Thus, for $BiFeO_3$ the temperature, after which the downward trend appears in the experimental dependence behavior, is 250 K. For sample $Bi_2Fe_4O_9$ this temperature reaches 300 K. This special point on the dependences seems to characterize the start of transformation of magnetic properties to the paramagnetic state. The experiment recorded different distribution by crystallite size in these samples (Figure 1, *b*). Wider distribution for sample $BiFeO_3$ explains the magnetic-ordered state of some of its substance at room temperature.

Therefore, the Arrhenius plotting of the function of $BiFeO_3$ and $Bi_2Fe_4O_9$ sample magnetization makes it possible to detect the presence of the maximum characterizing the start of transition of such materials to paramagnetic state. FC dependence on the opposite temperature may be described quantitatively by Hill model, the parameters of which enable comparison of magnetics with different composition and structure.

4. Conclusion

Using the glycine-nitrate combustion method, nanocrystalline materials based on $BiFeO_3$ and $Bi_2Fe_4O_9$ with crystallite sizes of 48 and 60 nm were synthesized. The samples have magnetic order at room temperature and higher magnetization compared to materials of similar composition. At 300 K and 20 kOe, the magnetization values for $BiFeO_3$ and $Bi_2Fe_4O_9$ are 1.2 and 2.5 emu/g, accordingly. It was shown that the temperature behavior of magnetization was quantitatively described by Hill model, the parameters of which found differences in values of the achieved maximum value of magnetization and nature of magnetic moments binding. The obtained result makes it possible to predict magnetic behavior of materials based on bismuth ferrites of various structure with temperature increase, which is useful for development of new magnetic media.

Acknowledgments

The authors thank Mikhail Pavlovich Volkov (Ioffe Institute) for sample magnetometry.

Conflict of interest

The authors declare that they have no conflict of interest.

References

[1] A.R. Akbashev, A.R. Kaul. Uspekhi khimii **80**, *12*, 1211 (2011). (in Russian).
[2] J. Wu, Zh. Fan, D. Xiao, J. Zhu, J. Wang. Progr. Mat. Sci. **84**, 335 (2016).
[3] T.-J. Park, G.C. Papaefthymiou, A.J. Viescas, A.R. Moodenbaugh, S.S. Wong. Nano Lett. **7**, 766 (2007).
[4] M. Pooladi, I. Sharifi, M. Behzadipour. Ceram. Int. **46**, 18453 (2020).
[5] I.E. Dzyaloshinski. ZhETF, **32**, 1547 (1957). (in Russian).
[6] T. Moriya. Phys. Rev. B **120**, 91 (1960).

[7] N.A. Lomanova, I.V. Pleshakov, M.P. Volkov, S.G. Yastrebov, K. Kenges, V.L. Ugolkov, A.V. Osipov, Siyuan Tao, I.V. Buryanenko, V.G. Semenov. Inorg. Chem. Commun. **161**, 112109 (2024).
[8] N.A. Lomanova, V.V. Panchuk, V.G. Semenov, I.V. Pleshakov, M.P. Volkov, V.V. Gusarov. Ferroelectrics **569**, *1*, 240 (2020).
[9] A.A. Ostroushko, I.D. Gagarin, E.V. Kudyukov, T.Yu. Zhulanova, A.E. Permyakova, O.V. Russkikh. Nanosyst.: Phys. Chem. Math. **14**, 571 (2023).
[10] T. Magno de Lima Alves, B.F. Amorim, M.A. Morales Torres, C.G. Bezerra, S.N. de Medeiros, P.L. Gastelois, L.E. Fernandez Outon, W.A. de Almeida Macedo. RSC Adv. **7**, 22187 (2017).
[11] N.S. Parvathy, R. Govindaraj. Sci. Rep. **12**, 4758 (2022).
[12] N.E. Gervits, A.V. Tkachev, S.V. Zhurenko, A.V. Gunbin, A.V. Bogach, N.A. Lomanova, D.P. Danilovich, I.S. Pavlov, A.L. Vasiliev, A.A. Gippius. Phys. Chem. Chem. Phys. **25**, *37*, 25526 (2023).
[13] S.A.N.H. Lavasani, O. Mirzaee, H. Shokrollahi, A.K. Moghadam, M. Salami Ceram. Int. **43**, 12120 (2017).
[14] Q. Zhang, W. Gong, J. Wang, X. Ning, Zh. Wang, X. Zhao, W. Ren, Zh. Zhang. J. Phys. Chem. C **115**, 25241 (2011).
[15] O.V. Proskurina, K.I. Babich, S.M. Tikhanova, K.D. Martinson, V.N. Nevedomskiy, V.G. Semenov, R.Sh. Abiev, V.V. Gusarov. Nanosystems: Phys. Chem. Math. **15**, *3*, 369 (2024).

Translated by M.Verenikina